We are IntechOpen,
the world's leading publisher of
Open Access books
Built by scientists, for scientists

4,800
Open access books available

122,000
International authors and editors

135M
Downloads

Our authors are among the

154
Countries delivered to

TOP 1%
most cited scientists

12.2%
Contributors from top 500 universities

CLARIVATE ANALYTICS
BOOK CITATION INDEX
INDEXED

WEB OF SCIENCE™

Selection of our books indexed in the Book Citation Index
in Web of Science™ Core Collection (BKCI)

Interested in publishing with us?
Contact book.department@intechopen.com

Numbers displayed above are based on latest data collected.
For more information visit www.intechopen.com

Chapter

Iron Oxides Synthesized in Hypersaline Solutions
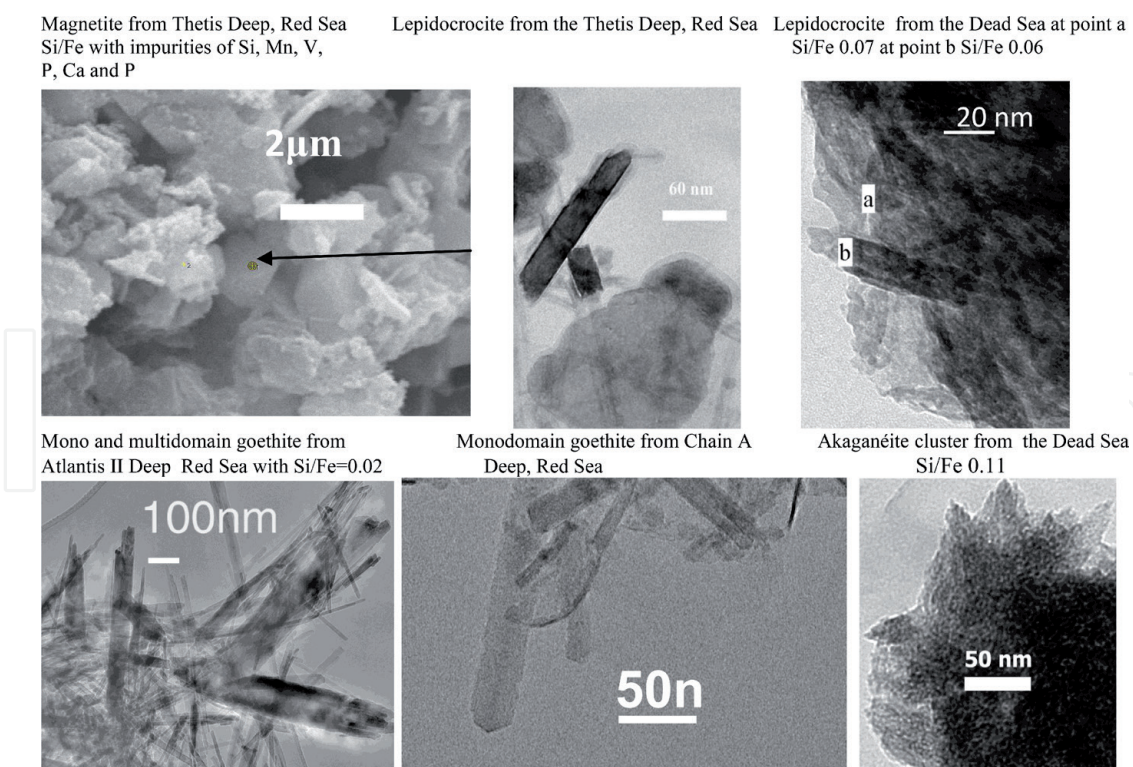
Nurit Taitel-Goldman

Abstract

Iron oxides were synthesized in conditions similar to those that prevail in deeps of the Red Sea (2–5M NaCl, temperatures 60–80°C, and pH 6.5–10.4). The main phase that was crystallized was submicron magnetite. Additional phases of feroxyhyte, goethite, and akagenéite were also detected. Magnetite morphology observed through high-resolution scanning electron microscopy (HRSEM) varied between euhedral plates and octahedral or unhedral crystals. The euhedral plates were probably crystallized pseudomorphically after platy green rust or $Fe(OH)_2$ due to its quick crystallization. Size of magnetite varied between 18 and 45 nm. The addition of Si retarded crystal growth, and at Si/Fe = 0.5, short-range ordered phases are formed and not magnetite. This finding is in line with earlier laboratory experiments in which Si was found to retard goethite and lepidocrocite crystallization.

Keywords: magnetite, HRSEM, hypersaline environment, feroxyhyte, goethite lepidocrocite, akagenéite

1. Introduction

Synthesis of iron oxides in hypersaline solutions was performed to imitate conditions that prevail in the Dead Sea and in deeps of the Red Sea. Salinity in the Dead Sea reaches 340 g/l. In the Red Sea, hydrothermal hypersaline brine discharges into the Atlantis II Deep with Cl concentrations in the upper layer of the brine at 67 g of Cl per kg of water (67 g/kg) and at the lower layer of the brine, 158 g/kg. The pH value decreases from 8.13 at RSDW to 5.2 at the lower layer [1]. The temperature of the lower layer is ~68°C measured in 2008 [2]. A narrow channel that connects the southern part of the Atlantis II Deep with the Chain Deeps enables overflowing of the brine of the lower convecting layer to Chain A, B, and C deeps. It was suggested that not only does the overflowing brine feed the adjacent deeps, but a fracture and fissure system enables a sub-bottom flow of the brine of the LCL from the Atlantis II Deep into the Chain and Discovery Deeps, leading to hydrothermal conditions in those deeps [1, 3]. The temperature in Chain A is 52.4–54°C; in Chain B, 46°C; in Chain C, 44.3°C; and in Discovery Deep, 44.7°C [4, 5]. There is no current hydrothermal activity in the Thetis Deep, yet it was active in the past but without a brine that filled the Deep [6].

Iron oxides (hematite-Fe_2O_3 and magnetite-Fe_3O_4), well-crystallized oxyhydroxides (goethite-$\alpha FeOOH$, lepidocrocite-$\gamma FeOOH$, feroxyhyte-$\delta FeOOH$, and akaganéite-$\beta FeOOH$), and short-range ordered oxyhydroxides (ferrihydrite-$Fe_5HO_8 \cdot 4H_2O$ and singerite-$SiFe_4O_6(OH)_4H_2O$) precipitated in the hypersaline environment of the Dead

Magnetite from Thetis Deep, Red Sea
Si/Fe with impurities of Si, Mn, V,
P, Ca and P

Lepidocrocite from the Thetis Deep, Red Sea

Lepidocrocite from the Dead Sea at point a
Si/Fe 0.07 at point b Si/Fe 0.06

Mono and multidomain goethite from
Atlantis II Deep Red Sea with Si/Fe=0.02

Monodomain goethite from Chain A
Deep, Red Sea

Akaganéite cluster from the Dead Sea
Si/Fe 0.11

Figure 1.
Pictures obtained by electron microscopy: Magnetite from the Thetis deep (scanning electron microscope (SEM)); lepidocrocite from the Thetis deep; lepidocrocite from the Dead Sea; mono- and multi-domain goethite from Atlantis II deep, Red Sea; mono-domain goethite from chain a deep, Red Sea; and cluster of akaganéite from the Dead Sea (high-resolution transmission electron microscope).

Sea and in the deeps of the Red Sea (Atlantis II, Chain A, Chain B, Discovery, and Thetis) [7–10] (**Figure 1**). Precipitation of these phases occurs at hypersaline environment with elevated temperatures and varying pH. Morphology of the crystals and their size is observed by high-resolution transmission electron microscopy (HRTEM). Using electron diffraction enables identifying the crystallographic structure. Goethite and lepidocrocite have orthorhombic structure, akaganéite has monoclinic structure, and feroxyhyte has hexagonal structure [11].

Short-range ordered ferrihydrite recrystallizes into well-crystallized phase, yet its initial morphology of plates at the size of <10 nm is preserved. Singerite (100 nm) disintegrates into iron-rich clay mineral [12]. Magnetite has a cubic morphology of octahedron or cubes 2–4 μm as observed in the Thetis Deep of the Red Sea.

Goethite has acicular form and changes at elevated pH from mono-domain to multi-domain rods. Crystal size at the Dead Sea area and the Red Sea varied from few 100 nm to 3 μm.

Lepidocrocite usually precipitates at fast oxidation rate at the presence of chloride, and its morphology changes from plates formed at lower pH to multi-domain rods that are formed at elevated pH. Lepidocrocite crystals size varied from 100 nm in the Dead Sea to 300 nm in the Red Sea deeps.

Rods and multi-domain akaganéite were observed at the Dead Sea with crystal size that varied from 100 nm to 1 μm.

Feroxyhyte plates are formed at very high oxidation rate and had a plate morphology with crystals size that reached 300 nm.

In earlier study, synthesis was performed imitating the upper convecting layer of the Atlantis II Deep with lower temperatures and salinity [13]. In this research, iron oxides were synthesized at higher pH, elevated temperatures, and hypersaline brines.

2. Methods

Iron oxides were synthesized under changing conditions of salinity, temperature, pH, and oxidation rates.

NaCl salt (Loba Chemie) was used to prepare NaCl solutions (2, 4, and 5M) that were used as a matrix and were kept in water bath at 40, 60, 70, and 80°C. Prior to synthesis, N_2 was bubbled through the solutions for 20 minutes to remove dissolved oxygen. pH buffering of the solutions was accomplished by adding either NaOH (Daejung) or $NaHCO_3$ (Carlo Erba) in small amounts, hence slightly changing Na concentration. pH of the solutions were 5.5, 7, 8.2, and 10.5. Cl concentration also changed due to dissolution of $FeCl_2 \cdot 4H_2O$ (Sigma-Aldrich) that was chosen for the Fe^{2+} solutions to yield a concentration of 0.06M.

Fe oxidation was carried out by introducing air at flow rates of 25, 40, 110, and 200 ml/min which was monitored with a flow meter and was kept stable during the hours of synthesis.

In order to isolate Si effects on the crystallization of iron oxides, Na_2SiO_3 (Sigma) was added to some of the solutions. To avoid any side effects, all of the samples were synthesized using the same polyethylene ware and under constant stirring speed. The precipitates were slightly washed and freeze-dried immediately after their synthesis.

Analyses of the precipitates were performed using X-ray diffraction (XRD).

The fitting of the peak profiles was performed by using Pseudo-Voigt function with the APD computer program developed by Philips Export B.V. A least square process using "Celsiz" software did the unit cell refinement.

Sample morphology was observed through transmission electron microscopy (TEM) and high-resolution scanning electron microscopy (HRSEM). Transmission electron microscopy was carried out on a JEOL FasTEM 2010 electron microscope equipped with the Noran energy dispersive spectrometer (EDS) for microprobe elemental analyses.

All chemical analyses were obtained by point analyses with beam width of 25 nm and are presented as atomic ratios. A NORAN Standardless Metallurgical Thin Films program based on the *Cliff-Lorimer* ratio technique with an accuracy of about 5% was used for calculations. CuK_α line was used for spectrometer calibration. Crystalline phases were identified using selected area electron diffraction (SAED) in the TEM.

3. Results and discussion

Initial identification of iron oxides was obtained by using X-ray diffractions (**Figure 2**). X-ray diffraction of all samples synthesized yielded the following results: At elevated temperatures, alkaline media and concentrated brine magnetite was the main phase that precipitated. At neutral to slightly acidic conditions, lepidocrocite, akaganéite, and goethite co-precipitated. Additional $NaHCO_3$ caused precipitation of siderite at 60°C.

In this study, pictures of iron oxides obtained by high-resolution scanning electron microscope and high-resolution transmission electron microscope are presented.

3.1 Magnetite FeO-Fe_2O_3

Unit cell parameters of magnetite vary from 0.8373 to 0.8396 nm with upper limit of 0.8396 nm, identical to that of well-crystallized magnetite [13]. Crystallite size changes from 18 to 45 nm. The smallest crystallites were obtained at pH 7.5 in 4 or 5M NaCl at all temperatures, whereas the largest crystallites were obtained at under elevated pH (9.5) and temperatures. The lowermost unit cell parameter was obtained for samples that crystallized at 60°C pH 8.5 and in 4M NaCl matrix. The largest unit
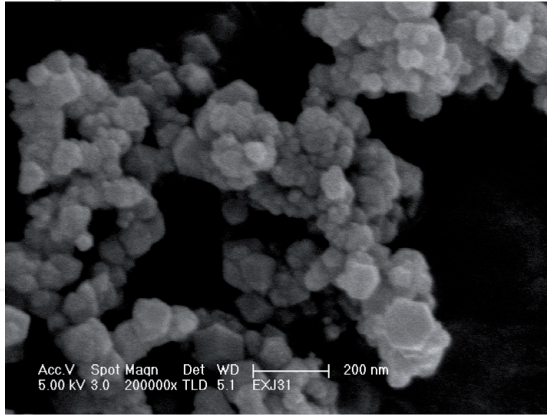
a

b
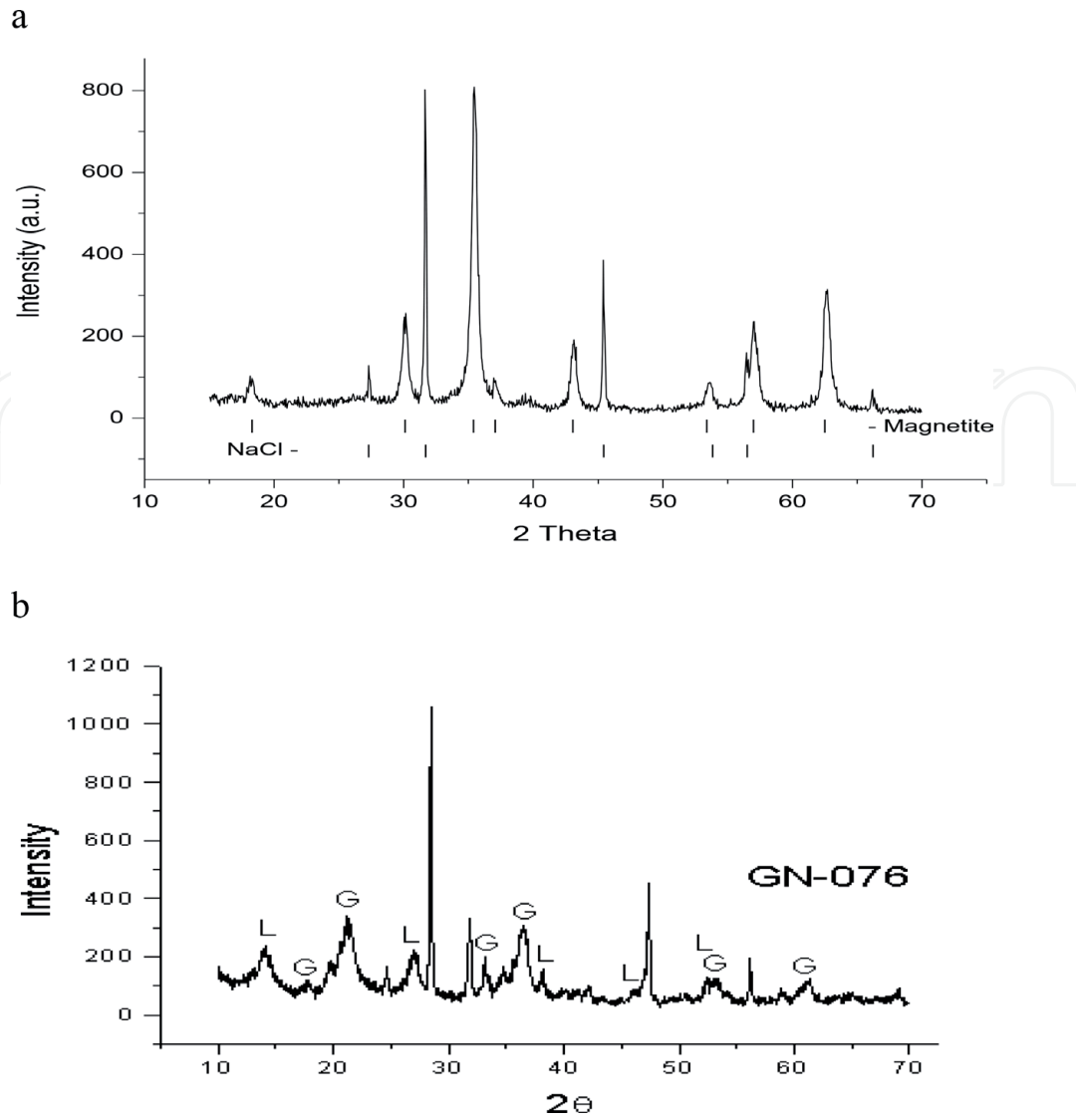
Figure 2.
X-ray diffraction patterns of (a) synthesized magnetite at 70°C, 5M NaCl, and pH 7.5; (b) goethite and lepidocrocite in sample from the Atlantis II deep, Red Sea.
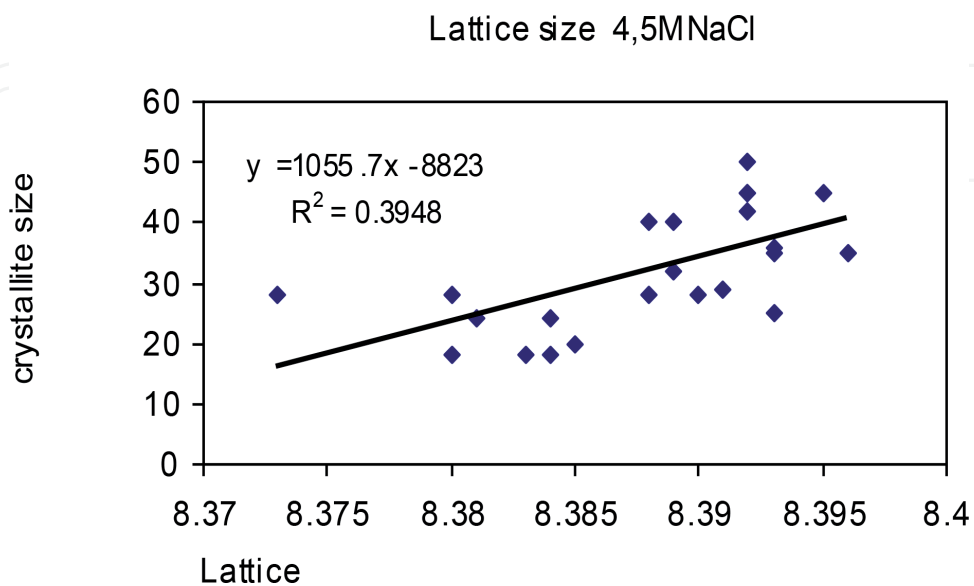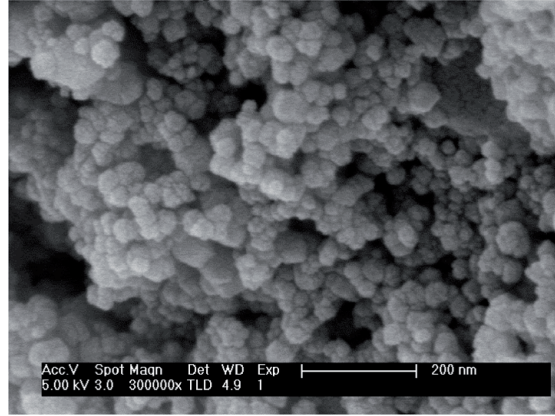

Figure 3.
Lattice parameter (nm) and crystalline sizes of magnetite precipitated in brines with concentrations of 4 and 5M NaCl.
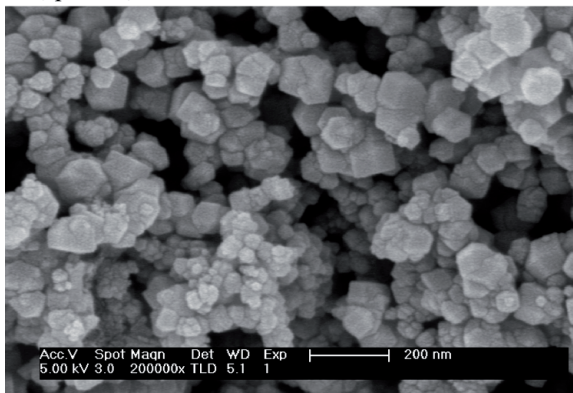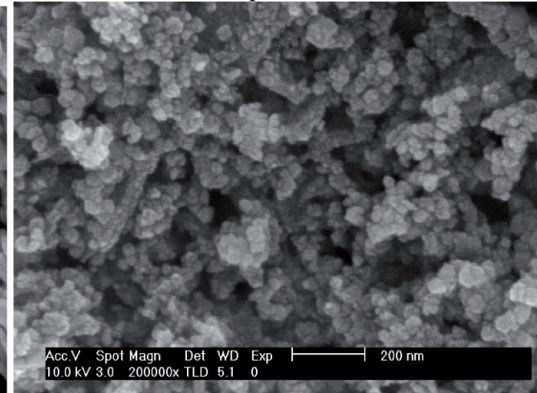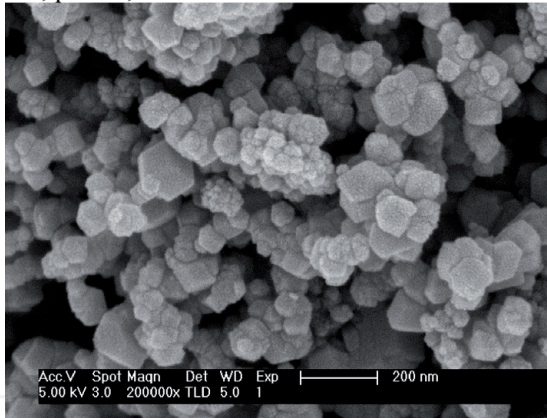
5M, pH 6.5, 80°C
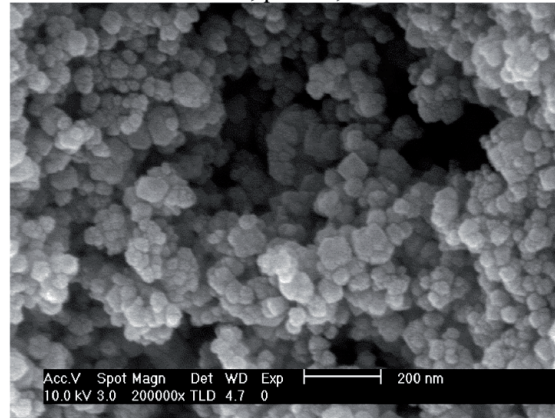
4M, pH 6.5, 80°C

5M, pH 6.5, 60°C

4M, pH 6.5, 70°C

5M, pH 6.5, 60°C

4M, pH 6.5,60°C

Figure 4.
Pictures obtained by HRSEM presenting the morphology of magnetite crystals precipitated at salinity of 4 and 5M NaCl, pH 6.5, and temperature of 60–80°C.

cell parameter was obtained for samples that crystallized under elevated pH 9.5, 5M NaCl and at 80°C. Overall, crystallite size and unit cell parameters were mainly affected by pH values, rather than by salinity or temperature changes (**Figure 3**).

Morphology of the crystals formed varied between unhedral to unhedral-octahedral, cubes, and hexagonal plates. The morphology of the crystals mainly results from the pH of the brines in **Figures 4–8**.

Magnetite Fe_3O_4: FeO-Fe_2O_3 crystallizes in cubic system with a = 0.8396 nm.

Crystallization from Fe^{2+} solutions usually involves crystallization of hexagonal flakes of $Fe(OH)_2$, which transforms to magnetite in moderately alkaline solutions (pH > 8). Under slightly acid to slightly alkaline conditions, green rust phases are formed, and upon further oxidation they are transformed into goethite and/or lepidocrocite [11]. Formation of magnetite in the hypersaline brines results from slow oxidation, elevated temperatures, and higher pH. The morphology of the magnetite
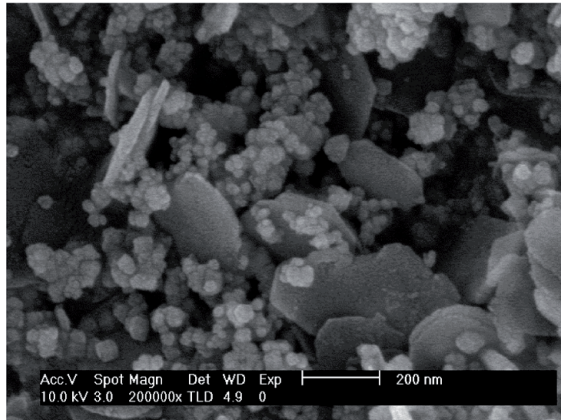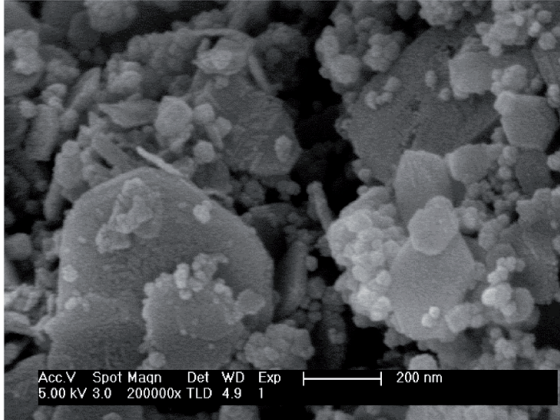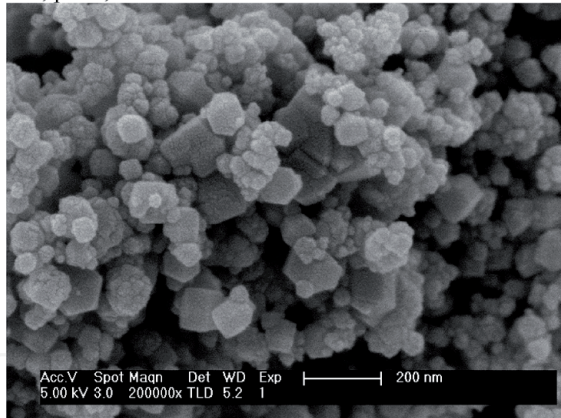
5
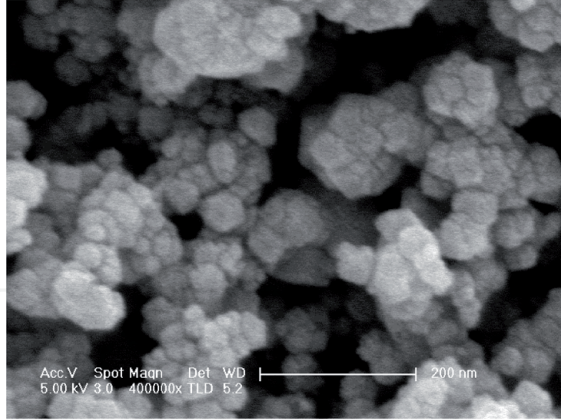
5M, pH 7.5, 80°C
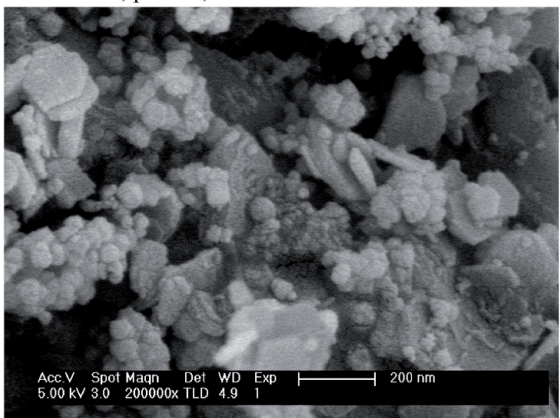
4M, pH 7.5, 80°C
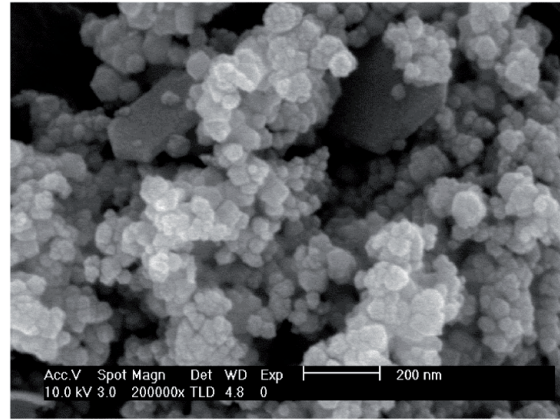
5M, pH 7.5, 70°C

4M, pH 7.5, 70°C

5M, pH 7, 60°C

4M, pH 7.5, 60°C

Figure 5.
Pictures obtained by HRSEM presenting the morphology of magnetite crystals precipitated at salinity of 4 and 5M NaCl, pH 7.5, and temperature of 60–80°C.

crystals was mainly affected by pH. In strongly alkaline brine, hexagonal flakes of $Fe(OH)_2$ were initially formed recrystallized into magnetite, preserving the initial morphology.

The morphology of magnetite of the Thetis Deep indicates that precipitation occurred at lower pH and lower salinity, suggesting that no brine pool filled the Thetis Deep [6].

3.2 Goethite (α-FeOOH)

Goethite precipitated along with other iron oxides. The morphologies of the crystals formed varied between mono-domain and multi-domain crystals. Twinning and star-shaped multi-domain crystals were formed at elevated temperatures. In higher salinity of 5M NaCl, goethite precipitated at pH 8.2 and 40°C, and at pH 7 and

5M, pH 8.5, 80°C

4M, pH 8.4, 80°C

5M, pH 8.5, 70°C

4M, pH 8.4, 70°C

5M, pH 8.4-8.5, 60°C

4M, pH 8.4, 60°C
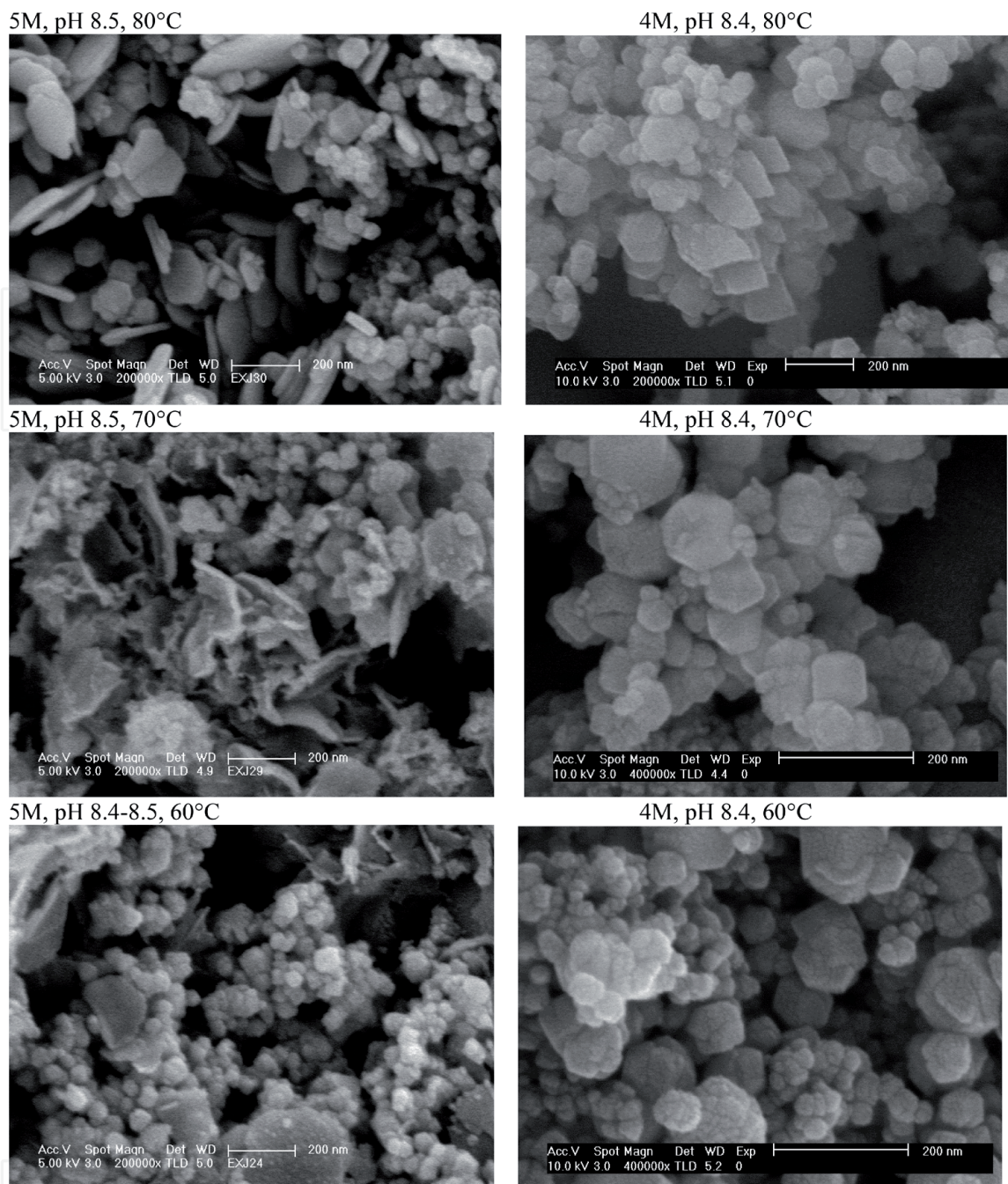
Figure 6.
Pictures obtained by HRSEM presenting the morphology of magnetite crystals precipitated at salinity of 4 and 5M NaCl, pH 8.5, and temperature of 60–80°C.

40°C, it co-precipitated with lepidocrocite and akaganéite. Adding $NaHCO_3$ to the solution caused co-precipitation of goethite with lepidocrocite at 40°C in 2M NaCl, co-precipitation of goethite with magnetite at 60°C and at 5M NaCl solutions, at pH 8.2, only magnetite precipitated magnetite [13] (**Figure 9**).

3.3 Lepidocrocite (γ-FeOOH)

Lepidocrocite precipitated at lower temperatures than magnetite. By using NaCl solutions of 5M and temperature of 40°C, the morphology of the crystals formed was affected by the pH. Plates crystallized at pH 5.5, rods at pH 7, and multi-domain crystals at pH 8.2 (**Figure 10**). The difference between the morphologies results from faster crystallization of 010 along c direction in crystals formed at higher pH leading to multi-domain crystals at pH 8.2. Similar results were also obtained at 25°C [13].

5M, pH 9.4, 80°C

4M, pH 9.4, 80°C

5M, pH 9.4, 70°C

4M, pH 9.4, 70°C

5M, pH 9.4, 60°C

4M, pH 9.4, 60°C
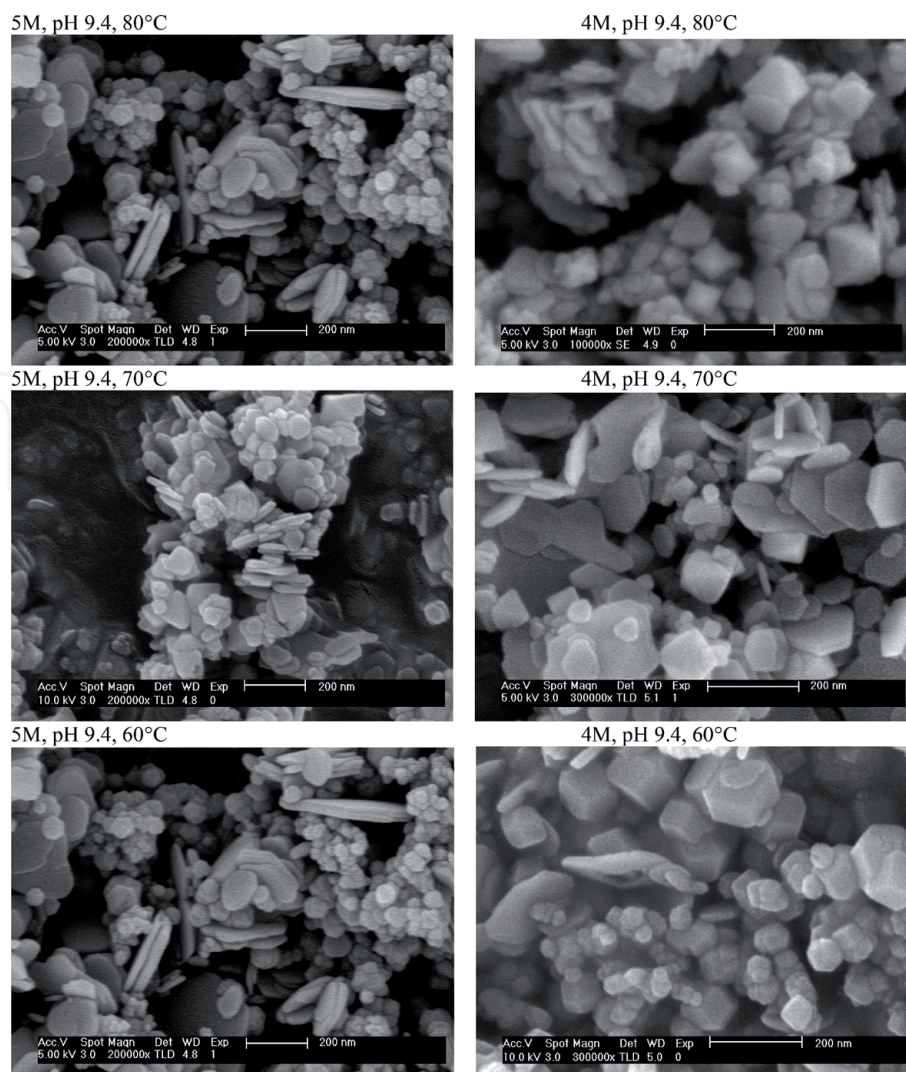
Figure 7.
Pictures obtained by HRSEM presenting the morphology of magnetite crystals precipitated at salinity of 4 and 5M NaCl, pH 9.4, and temperature of 60–80°C.
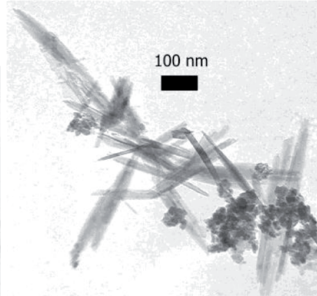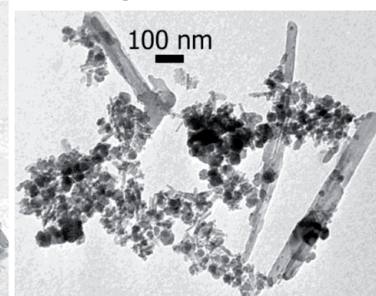
4M pH 10, 60°C

5M pH 10, 60°C

4M pH 10, 60°C

5M pH 10 70°C
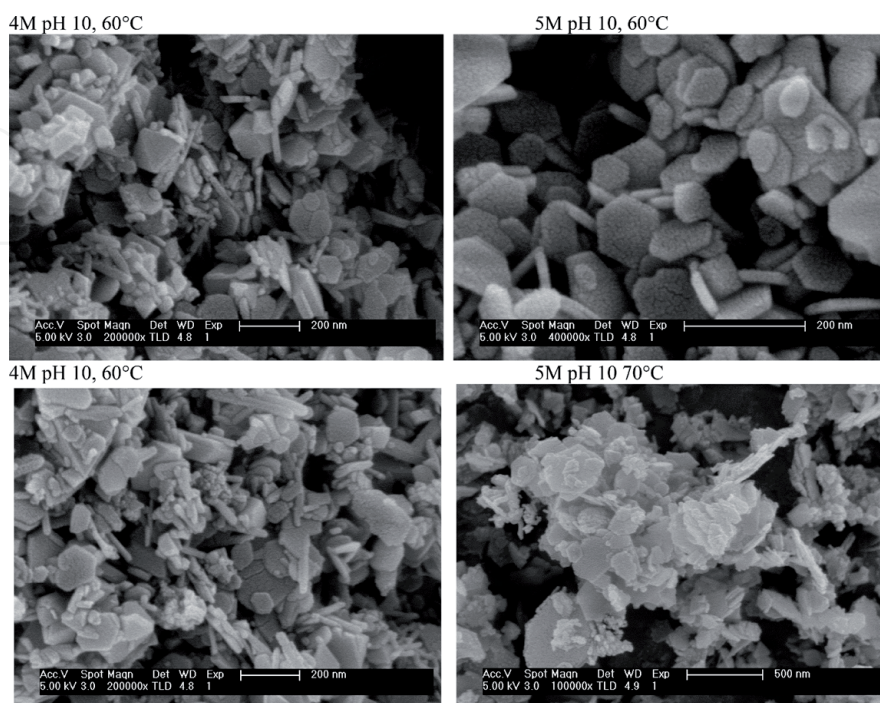
Figure 8.
Pictures obtained by HRSEM presenting the morphology of magnetite crystals precipitated at salinity of 4 and 5M NaCl, pH 10, and temperature of 60–70°C.
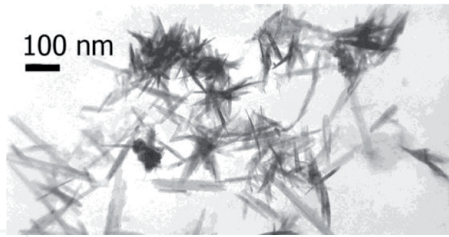
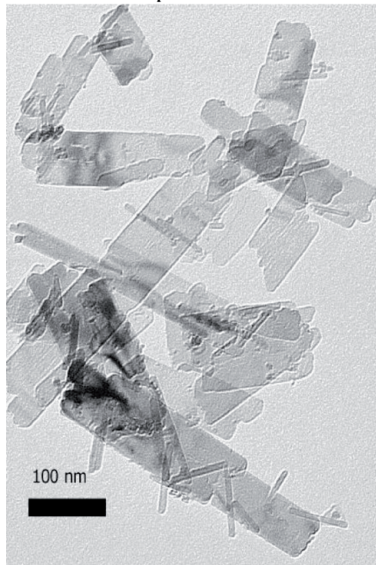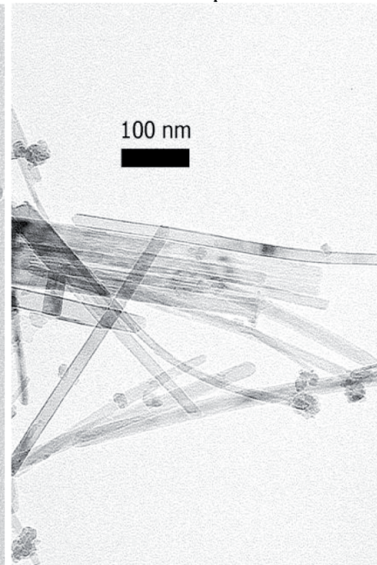2M NaCl 40°C NaHCO₃   5M NaCl 40°C NaHCO₃   5M 40°C pH 8.2

Figure 9.
Goethite crystals observed through HRTEM. The crystals were synthesized at 40°C, in solutions of 2 and 5M NaCl and with additional NaHCO₃ or at pH 8.2.
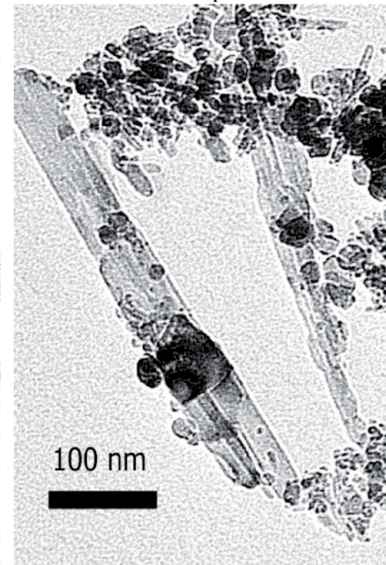
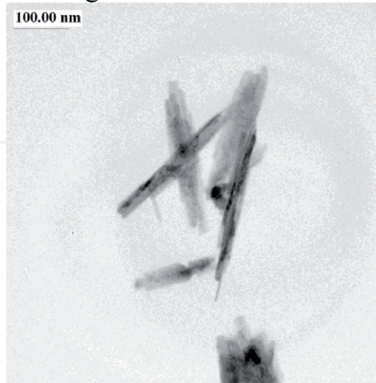5M 40°C pH 5.5   5M 40°C pH 7   5M 40°C pH 8.2
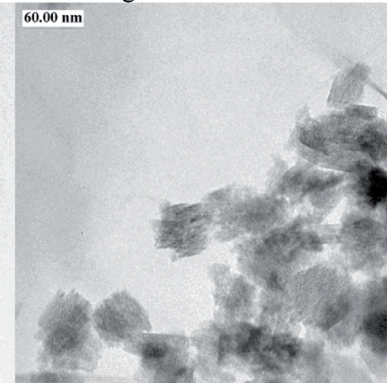

Figure 10.
Lepidocrocite crystals observed through TEM. Crystals were formed in NaCl solutions of 5M concentration at 40°C and pH 5.5, 7, and 8.2. At pH 8.2 magnetite crystals co-precipitated with multi-domain lepidocrocite.

40°C 2MNaCl and 1N NaHCO₃
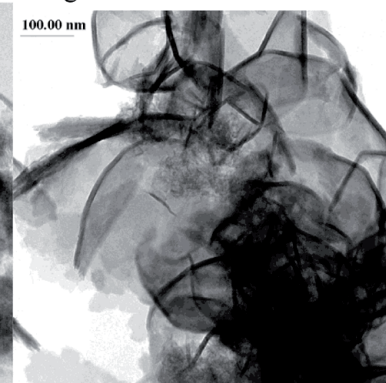0.0135gr Na₂SiO₃H₂O   0.135gr Na₂SiO₃H₂O   1.35gr Na₂SiO₃H₂O

Figure 11.
Pictures obtained by HRTEM presenting the effect of additional Na₂SiO₃H₂O to solution of 4M NaCl, at 40°C.

3.4 Effect of additional Si

Addition of $Na_2SiO_3H_2O$ into the solutions was selected to see the effect of Si on iron oxide crystallization. In precipitation of magnetite crystals, $Na_2SiO_3H_2O$ was added to a solution of 4M NaCl, pH 7.5 at a temperature of 60°C. The presence of Si

affected crystal size, which became smaller, from 30 to 26 nm, and unit cell parameter decreased from 0.8392 to 0.8380 nm.

Addition of 0.0135 g $Na_2SiO_3H_2O$ to the solutions at the initial crystallization stage hindered crystal growth of goethite crystals (**Figure 11**). Elevated amounts of Si added as 0.135 g Na_2SiO_3 and 1.35 g caused formation of short-range ordered phases (suggested name singerite) [12].

4. Conclusions

Magnetite crystalized in hypersaline 2–5M brine at elevated temperatures 60–80°C and pH 6.5–10. At high alkalinity, their initial formation stage of hexagonal plates was preserved. At lower alkalinity, their morphology was unhedral cubes. Additional Si to the brines caused smaller crystals.

Lepidocrocite and goethite were formed at lower temperatures (40°C). High alkalinity effected crystal morphologies causing multi-domain structure in goethite and in lepidocrocite and twinning formation.

Additional Si hindered crystal growth.

Author details

Nurit Taitel-Goldman
The Open University of Israel, Raanana, Israel

*Address all correspondence to: nuritg@openu.ac.il

IntechOpen

References

[1] Hartmann M, Scholten JC, Stoffers P, Wehner F. Hydrographic structure of brine-filled deeps in the Red Sea—New results from the Shaban, Kerbit, Atlantis II, and discovery deep. Marine Geology. 1998a;**144**:311-330

[2] Swift A, Bower AS, Schmitt R. Vertical, horizontal, and temporal changes in temperature in the Atlantis II and discovery hot brine pools, Red Sea. Deep Sea Research Part I: Oceanographic Research Papers. 2012;**1**(64):118-128

[3] Pierret MC, Clauer N, Bosch D, Blanc C, France-Lanord C. Chemical and isotopic (87Sr/86Sr, d18O, dD) constraints in the formation processes of Red Sea brines. Geochimica et Cosmochimica Acta. 2001;**65**:1259-1275

[4] Ramboz C, Danis M. Superheating in the Red Sea? The heat-mass balance of the Atlantis II deep revisited. Earth and Planetary Science Letters. 1990;**97**:190-210

[5] Hartmann M, Scholten JC, Stoffers P. Hydrographic structure of brine-filled deeps in the Red Sea: Correction of Atlantis II deep temperatures. Marine Geology. 1998b;**144**:331-332

[6] Pierret MC, Clauer N, Bosch D, Blanc G. Formation of Thetis deep metal-rich sediments in the absence of brines, Red Sea. Journal of Geochemical Exploration. 2010;**104**:12-26

[7] Taitel-Goldman N, Bender-Koch C, Singer A. Lepidocrocite in hydrothermal sediments of the Atlantis II and Thetis deeps, Red Sea. Clays and Clay Minerals. 2002;**50**:186-197

[8] Taitel-Goldman N, Bender-Koch C, Singer A. Si-associated goethite in hydrothermal sediments of the Atlantis II and Thetis deeps, Red Sea. Clays and Clay Minerals. 2004;**52**:115-129

[9] Taitel-Goldman N, Ezerski V, Mogilyanski D. High resolution transmission electron microscopy study of Fe-Mn oxides in the hydrothermal sediments of the Red Sea deeps system. Clays and Clay Minerals. 2009;**57**:465-475

[10] Taitel-Goldman N, Ezerski V, Mogilyanski D. Nano-sized iron-oxides in the Dead Sea area. Journal of Earth Science. 2016;**2**:94-104

[11] Cornell RM, Schwertmann U. The Iron Oxides: Structure, Properties, Reactions, Occurrences. Weinheim, Germany: Wiley VCH; 2003

[12] Taitel-Goldman N, Singer A. Metastable Si-Fe phases in hydrothermal sediments of Atlantis II deep, Red Sea. Clay Minerals. 2002;**37**:235-248

[13] Taitel-Goldman N, Singer A. Synthesis of clay-sized iron oxides under marine hydrothermal conditions. Clay Minerals. 2002;**37**:719-731